03.2

Hydrodynamic heat transfer localization in impinging gas jet

© V.V. Lemanov, V.V. Lukashov, K.A. Sharov

Kutateladze Institute of Thermophysics, Siberian Branch, Russian Academy of Sciences, Novosibirsk, Russia
E-mail: lemanov@itp.nsc.ru

Received August 8, 2023
Revised November 29, 2023
Accepted November 29, 2023

The results of an experimental study of heat transfer in an impinging air jet flowing from a long round channel in the range of Reynolds numbers 250−10000 are presented. Data on local heat transfer in the region of the flow stagnation point at large distances to the barrier ($h/d = 20$) were obtained. It is shown that a more localized heat flow corresponds to a laminar flow in a jet source compared to the case of a turbulent regime in the source. The maximum heat transfer is achieved not for the Poiseuille profile in the channel, but in the case of a transition regime with a small percentage of turbulent vortex structures.

Keywords: impinging jet, heat transfer, laminar-turbulent transition, vortex structure.

DOI: 10.61011/PJTF.2024.05.57183.19704

The issue of spatial localization of transfer processes in jet flows has been examined in various fluid and gas flows. The phenomenon of a cumulative jet with spatial localization of a gas flow at high velocities is known in gas dynamics [1]; aerodynamic focusing in low-density gases has also been observed [2]. The issue of flow focusing has been studied extensively in microhydrodynamics [3].

The known problem of heat transfer enhancement within a localized region of a surface in a flow is especially relevant to MEMS (micro-electromechanical systems) devices [4]. The heat transfer process is focused in this context through the use of, e.g., micrometer-sized impinging jets and correspondingly low Reynolds numbers [5]. It has been demonstrated earlier that the optimum configuration for heat transfer enhancement within the wall-adjacent region of impinging macrojets is the one with shaped contractors, high Reynolds numbers ($\mathrm{Re} > 10^4$), and short distances to the barrier $h = (4-6)d$ [6,7], where d is the nozzle diameter. With these parameters, the heat transfer reaches a slight maximum at the stagnation point and is distributed smoothly over the barrier radius. A profound heat transfer enhancement (upward of 300%) at the stagnation point has been observed in experiments [8] for a jet flowing from a long pipe at low Reynolds numbers ($\mathrm{Re} < 4000$), but the mechanism of this effect has barely been investigated. The present study is focused on the issue of spatial localization of heat transfer in the wall-adjacent region of impinging air macrojets at large distances to the barrier ($h/d > 10$). The possibility of localization of heat transfer in the wall-adjacent region of a jet flowing from a shaped nozzle is also examined.

The experimental setup included a gas line (a compressed air source, flexible hoses, a flow meter, and a jet source) and a heat transfer section. The following jet sources were used: (1) a brass pipe with diameter $d = 3$ mm and length $l = 1$ m; (2) a photopolymer shaped contractor (Vitoshinsky nozzle) with diameter $d = 3$ mm and a contraction ratio of 16. Outflow into the ambient air environment at room conditions was examined. A two-axis traversing device with a minimum pitch of 0.05 mm was used to shift the jet source. The distance from the jet origin to the plate was $h = 60$ mm ($h/d = 20$). The heat transfer section (copper plate 190 mm in diameter and 50 mm in thickness) was heated by an electric heater. Six film heat flow probes (HFPs) $2 \times 2 \times 0.2$ mm in size were positioned along the radius of jet spillage over the surface. These HFPs had a temporal resolution as fine as 3−4 kHz [9] and were connected to a computer via a multichannel amplifier and an analog-to-digital converter. Each time realization of instantaneous heat flow density Q' from a single HFP included $10^4-2 \cdot 10^5$ values. The mean value of heat flow density (Q) and the root-mean-square value of heat flow density pulsations (q) were then calculated. The measurement interval was 3−60 s. The experiment was performed at various fixed surface temperatures $T_w = \mathrm{const}$ of the heat transfer section within the temperature interval of 40−50°C. The results at each spatial point were averaged over an ensemble of ten experimental realizations for a given fixed T_w. Experiments on heat transfer at the stagnation point were carried out with the use of two different HFPs. The intrinsic uncertainty of measurement of the instantaneous heat flow density value was 2−4% [9].

The mean value of heat transfer coefficient α was determined from Q and the difference between wall T_w and jet T_j temperatures. The air parameters (kinematic viscosity ν and thermal conductivity λ) needed for calculation of Reynolds $\mathrm{Re} = Ud/\nu$ and Nusselt $\mathrm{Nu}_0 = \alpha d/\lambda$ numbers were determined based on the nozzle-exit flow temperature (U is the mean-flow-rate velocity). The instantaneous heat flow value, the gas flow rate, temperatures of the plate and the jet at the initial cross section, and the barometric pressure were measured in experiments on heat transfer. Dynamic jet parameters were determined using a DISA55M hot-wire anemometer and a 55P11 small-scale probe.

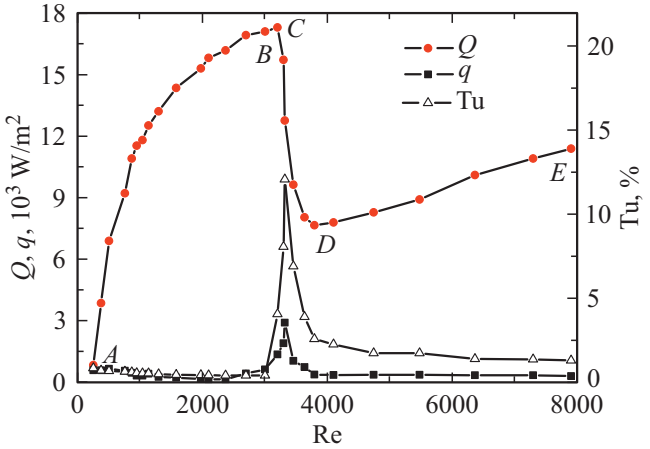

Figure 1. Dependences of the mean value of heat flow density Q, the root-mean-square value of heat flow density pulsations q, and turbulence level Tu on Reynolds number Re.

The results of examination of an impinging jet flowing from a long pipe are presented in Fig. 1. The variation of parameters Q and q at the stagnation point and turbulence level $\mathrm{Tu} = (u/U) \cdot 100\%$ at the pipe exit with Reynolds number (u is the root-mean-square value of the longitudinal velocity pulsation component). The flow in an impinging jet was characterized according [10] to the flow regime in the jet source (pipe): laminar, transition, or turbulent. The transition pipe flow regime was identified by visualizing and detecting large-scale turbulent structures (puffs) with the hot-wire anemometer [10,11]. Segment $A-B$ ($\mathrm{Re} = 250-3004$) in Fig. 1 is distinguished by a monotonic Q growth and low levels of q and Tu. The flow in a laminar jet is characterized by instability in the mixing layer [12,13]. The region of transition to turbulence is located at $h/d > 20$; the initial jet velocity profile corresponds to the Poiseuille distribution [10]. Segment $B-D$ ($\mathrm{Re} = 3004-3796$) with a laminar–turbulent transition in the pipe is distinguished by a significant Q reduction and high levels of q and Tu. The flow motion in a transition jet is characterized by intermittency: the flow is laminar at times and turbulent at other times. Turbulent segment $D-E$ ($\mathrm{Re} = 3796-7900$) features a monotonic insignificant Q growth and low levels of q and Tu.

The distribution of mean heat flow density along radius r at the plate for two flow regimes in an impinging jet is presented in Fig. 2. These data were obtained by performing a separate series of experiments for laminar flow at $\mathrm{Re} = 1920$ and turbulent flow at $\mathrm{Re} = 4240$. The plotted data points correspond to different positions of the jet source, which was shifted with respect to the heater axis using the traversing device. The axial symmetry of flow in the wall-adjacent region of an impinging jet was verified in these experiments by monitoring the axial symmetry of the radial distribution of mean heat flow density and by performing additional measurement of the velocity field via particle image velocimetry (PIV). For ease of comparison, the data in Fig. 2 are presented in dimensionless form Q/Q_0, where Q and Q_0 are the heat flow densities at arbitrary radius r and stagnation point $r = 0$, respectively. It can be seen that the radial distribution of heat flow in the laminar regime (segment $A-B$ in Fig. 1) is more localized around the stagnation point ($r/d = 0$) than the distribution for turbulent flow (segment $D-E$ in Fig. 1). It has been determined in earlier measurements of the velocity profile that the opening angle is $3-6^\circ$ in a laminar jet and $20-26^\circ$ in a turbulent jet [10].

The regimes of heat transfer in an impinging jet corresponding to different jet sources (a pipe and a contractor) are compared in Fig. 3 in the form of dependences $\mathrm{Nu}_0 = f(\mathrm{Re})$ plotted at fixed parameter values ($d = 3$ mm, $h/d = 20$). Correlation dependence $\mathrm{Nu}_0 = 5.25\mathrm{Re}^{0.5}\mathrm{Pr}^{0.33}(h/d)^{0.77}$ [6] is shown with a straight line in the same figure for comparison. It is evident that the heat transfer at the stagnation point intensifies monotonically in the case of a jet outflowing from a nozzle, following correlation $\mathrm{Nu}_0 \sim \mathrm{Re}^{0.5}$. At the same time, the heat transfer for an impinging jet outflowing from a long pipe behaves non-monotonically at $\mathrm{Re} < 4000$. The Nusselt number for a jet from a pipe is maximized (point C in Fig. 3) at $\mathrm{Re} = 3202$. This maximum corresponds to the extremal value of mean heat flow density Q (point C in Fig. 1). In the case of outflow from a pipe, the Nusselt number increases significantly (by up to 300%) within the $\mathrm{Re} = 400-3800$ range compared to a jet outflowing from a nozzle. At $\mathrm{Re} > 4000$, the difference in heat transfer between these two jet formation mechanisms (outflow from a pipe and a nozzle) becomes virtually nonexistent. The experimental data for microjets [5] at low Reynolds numbers deviate substantially from the known correlation dependence ($\mathrm{Nu}_0 \sim \mathrm{Re}^{0.5}$) typical of impinging macrojets.

It is known that the initial conditions exert a significant influence on jet flows [12,13]. It has been demonstrated ear-

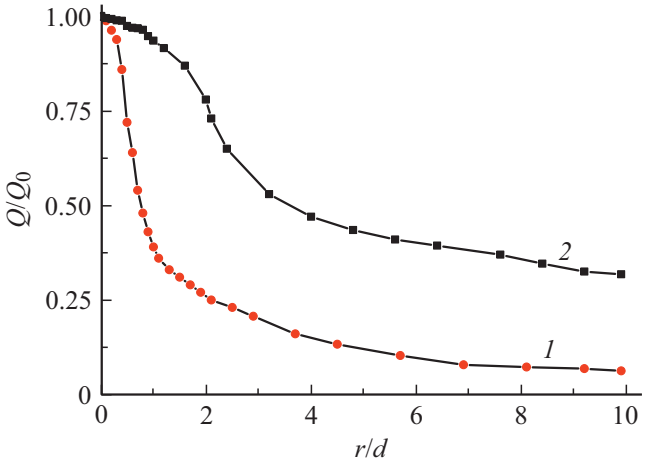

Figure 2. Distributions of the mean heat flow density in an impinging jet along the plate radius (pipe, $d = 3$ mm, $h/d = 20$). *1* — laminar regime ($\mathrm{Re} = 1920$, $T_w = 46.8^\circ$C, and the opening angle is $3-4^\circ$); *2* — turbulent regime ($\mathrm{Re} = 4240$, $T_w = 47.1^\circ$C, and the opening angle is $22-24^\circ$.

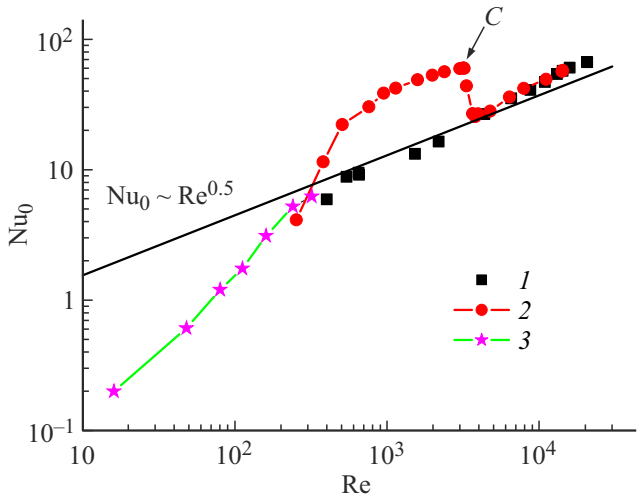

Figure 3. Heat transfer at the stagnation point in interaction between an impinging jet and a plane barrier. Points *1–3* — experiment: *1* — nozzle, $d = 3$ mm, $h/d = 20$; *2* — pipe, $d = 3$ mm, $h/d = 20$; *3* — microjet [5]. The straight line represents the correlation dependence [6].

lier that an initial parabolic velocity law is conducive to an increase in the coordinate value corresponding to the transition to turbulence in laminar flows ($x/d = 100–200$ — „long-range“ effect) [10,14,15]. At the same time, an initial velocity profile forming in outflow from a contractor („impact“ profile with thin boundary layers) induces a rapid transition to turbulence ($x/d = 2–6$) [12,16]. The jet turbulent section has a large opening angle ($15–26^\circ$) in the case of outflow both from a contractor [13] and a pipe [10]. With impinging jets, this results in cooling of a large area and a more uniform distribution along the barrier radius. Thus, the effect of heat transfer localization at distances $h/d > 4–6$ is not achieved in outflow from contractors of this type. A large coordinate value corresponding to the transition to turbulence in outflow from a long pipe [14] provides an opportunity to form a laminar impinging jet with a small opening angle, which induces a more spatially constrained thermal interaction with the barrier. Owing to this, the mean heat flow at the stagnation point within segment $B–C$ is greater than the one within segment $D–E$ (Fig. 1). The question remains open of whether a long pipe is a better choice for heat transfer localization within the wall-adjacent region of an impinging jet than an arbitrarily-shaped contractor.

However, the maximum mean value of heat flow (point C in Fig. 1) or the Nusselt number (point C in Fig. 3) for outflow from a long pipe corresponds to the laminar–turbulent transition region ($\mathrm{Re} = 3202$). Thus, the maximum heat transfer intensity is not achieved with an initial Poiseuille profile. It is known that the laminar–turbulent transition in pipes involves intermittency with large-scale vortex structures (puffs) forming and vanishing in turns [11]. In the experiment in question (point C in Fig. 1), the share of turbulent structures is approximately 10%. The effect of these large-scale structures on heat transfer warrants further study.

The integrated heat transfer for the whole heated surface is another practically relevant matter. Since the effect of heat transfer localization is related to the initial jet size, a system of jets is apparently needed for efficient cooling of surfaces of a significantly greater area. The above-described mechanism of heat transfer localization in the wall-adjacent region is driven by a hydrodynamic process (i.e., a change in the flow regime) instead of a variation of geometric pipe parameters. In our view, similar local heat transfer intensification may be achieved with both round and plane gas jets, since the „long-range“ effect [14,15] and small opening angles are present in both cases. The extension of this localization mechanism to momentum, heat, and mass transfer processes in the wall-adjacent region of inert and interacting impinging jets is also a promising research direction. The obtained results may be of use in the design of advanced heat exchangers.

Funding

This study was supported financially by the Russian Science Foundation (grant No. 23-29-00584).

Conflict of interest

The authors declare that they have no conflict of interest.

References

[1] B.V. Rumyantsev, S.I. Pavlov, Tech. Phys. Lett., **46**, 843 (2020). DOI: 10.1134/S1063785020090102.
[2] J.F. de la Mora, J. Rosell-Llompart, J. Chem. Phys., **91**, 2603 (1989). DOI: 10.1063/1.456969
[3] S.L. Anna, N. Bontoux, H.A. Stone, Appl. Phys. Lett., **82**, 364 (2003). DOI: 10.1063/1.1537519
[4] B. Dash, J. Nanda, S.K. Rout, Heat Transfer, **51**, 1406 (2022). DOI: 10.1002/htj.22357
[5] C.J. Chang, H. Chen, C. Gau, Nanoscale Microscale Thermophys. Eng., **17**, 92 (2013). DOI: 10.1080/15567265.2012.761304
[6] B.N. Yudaev, M.S. Mikhailov, V.K. Savin, *Teploobmen pri vzaimodeistvii strui s pregradami* (Mashinostroenie, M., 1977) (in Russian).
[7] S.D. Barewar, M. Joshi, P.O. Sharma, P.S. Kalos, B. Bakthavatchalam, S.S. Chougule, K. Habib, S.K. Saha, Therm. Sci. Eng. Prog., **39**, 101697 (2023). DOI: 10.1016/j.tsep.2023.101697
[8] V.V. Lemanov, V.I. Terekhov, High Temp., **54**, 454 (2016). DOI: 10.1134/S0018151X1603010X.
[9] S.Z. Sapozhnikov, V.Yu. Mityakov, A.V. Mityakov, *The science and practice of heat flux measurement* (Springer Nature, 2020).
[10] V.V. Lemanov, V.V. Lukashov, K.A. Sharov, Fluid Dyn., **55**, 768 (2020). DOI: 10.1134/S0015462820060087.

[11] K. Avila, D. Moxey, A. Lozar, M. Avila, D. Barkley, B. Hof, Science, **333**, 192 (2011). DOI: 10.1126/science.1203223
[12] C.M. Ho, P. Huerre, Annu. Rev. Fluid Mech., **16**, 365 (1984). DOI: 10.1146/annurev.fl.16.010184.002053
[13] A.S. Ginevsky, Ye.V. Vlasov, R.K. Karavosov, *Acoustic control of turbulent jets* (Springer, Berlin–Heidelberg, 2004).
[14] V.V. Lemanov, V.I. Terekhov, K.A. Sharov, A.A. Shumeiko, Tech. Phys. Lett., **39**, 421 (2013). DOI: 10.1134/S1063785013050064.
[15] V.M. Aniskin, V.V. Lemanov, N.A. Maslov, K.A. Mukhin, V.I. Terekhov, K.A. Sharov, Tech. Phys. Lett., **41**, 46 (2015). DOI: 10.1134/S1063785015010034.
[16] C. Bogey, C. Bailly, Phys. Fluids, **18**, 065101 (2006). DOI: 10.1063/1.2204060

Translated by D.Safin